Journal of Molecular Graphics and Modelling 27 (2009) 881–888

Contents lists available at ScienceDirect

Journal of Molecular Graphics and Modelling

journal homepage: www.elsevier.com/locate/JMGM

# Comprehensive structural characterization of the cyclic disulphide-bridged nonapeptides, Arg- and Lys-conopressins

Gábor Janzsó [a], Gábor Rákhely [a,b], Balázs Leitgeb [a,*]

[a] Institute of Biophysics, Biological Research Center of the Hungarian Academy of Sciences, Temesvári krt. 62, H-6726 Szeged, Hungary
[b] Department of Biotechnology, University of Szeged, Középfasor 52, H-6726 Szeged, Hungary

ARTICLE INFO

*Article history:*
Received 24 November 2008
Received in revised form 21 January 2009
Accepted 23 January 2009
Available online 3 February 2009

*Keywords:*
Conopressin
Conformational analysis
*Cis–trans* isomerization
Conformational space
Ramachandran plot
Turn structure
Intramolecular H-bond

ABSTRACT

Arg-conopressin-S and Lys-conopressin-G are cyclic disulphide-bridged nonapeptides isolated from the venom of cone snails. We performed a comprehensive conformational analysis for the *cis* and *trans* isomers of these conopeptides, in order to identify their characteristic structural and conformational features. In the course of our theoretical study, the Φ–Ψ and $\chi_1$ conformational spaces were explored in detail and the conformational distributions were compared to each other. For both *cis* and *trans* isomers of conopressins, the characteristic secondary structural elements and intramolecular H-bonds were identified. Our results pointed out that various turn structures stabilized by typical intramolecular H-bonds could be observed in the conformers of these conopeptides. Comparing the different conformational features of the *cis* and *trans* isomers of conopressins disclosed that several of them could be found for both isomers, however, structural properties characteristic for only the *cis* or *trans* isomer were also identified. Altogether, our comprehensive conformational study provided a detailed description of the three-dimensional (3D) structure of both conopressins.



## 1. Introduction

Arg-conopressin-S (Arg-CP-S, H-Cys-Ile-Ile-Arg-Asn-Cys-Pro-Arg-Gly-$NH_2$) and Lys-conopressin-G (Lys-CP-G, H-Cys-Phe-Ile-Arg-Asn-Cys-Pro-Lys-Gly-$NH_2$) are cyclic nonapeptides, which were isolated from the venom of fish-hunting cone snails, *Conus striatus* and *Conus geographus*, respectively [1]. These two conopeptides consist of a cyclic structure formed by a disulphide bridge between the $Cys^1$ and $Cys^6$ residues, as well as of a remaining C-terminal tripeptide tail. Nevertheless, they are characterized by an amidated C-terminal end and they contain two basic amino acids: one of them (*i.e.* Arg) in position 4 of the hexapeptide ring, and another (*i.e.* Arg or Lys) in position 8, outside of the cyclic structure.

These two conopressins were first isolated as invertebrate vasopressin/oxytocin-related peptides, and they induced an intense scratching effect in the injected mice [1]. Both conopeptides were found to be secreted by the neuronal tissue of venom duct, and they were assumed to play a role in the envenomation process [1,2]. Studies performed on the Lys-CP-G isolated from *Lymnaea stagnalis* revealed that this peptide possessed neurotransmitter and neuromodulator effects, namely, it caused muscular contraction of vas deferens, and it inhibited central neurons controlling female reproductive behavior [3,4]. Moreover, two G-protein-coupled receptors (*i.e.* LSCPR1 and LSCPR2) were identified for the Lys-CP-G in *Lymnaea stagnalis*, which seemed to mediate both vasopressin-like metabolic and oxytocin-like reproductive functions of this conopeptide [4,5].

Although, the physiological properties and biological effects of Arg- and Lys-conopressins have been examined in detail, to the best of our knowledge, any data derived either from experimental or from theoretical investigations, concerning the three-dimensional (3D) structure of these conopeptides, have not been published in the literature, so far. However, for other two conopressins (*i.e.* γ-conopressin-vil, γ-CP-vil; and conopressin-T, CP-T) isolated from the venom of *Conus villepinii* and *Conus tulipa*, respectively, structural data are available in the literature [6,7]. Based on the NMR spectra, γ-CP-vil was found to be very flexible in solution, irrespective of the applied temperature and medium [6]. In contrast, in the case of CP-T and its L7P-CP-T analog, the $^1$H NMR measurements combined with simulated annealing (SA) and molecular dynamics calculations indicated a well-defined structure for the cyclic hexapeptide ring, as well as a disordered structure for the C-terminal tripeptide tail [7]. On the basis of this study, moreover, it was concluded that these two peptides are mainly characterized by a β-turn structure located in the tetrapeptide unit covering residues 4–7.

Since any structural data could not be found in the literature for Arg- and Lys-conopressins, therefore, the aim of our theoretical study was to perform a comprehensive conformational analysis on these two conopeptides. Nevertheless, our further aim was to

* Corresponding author. Tel.: +36 62 599 726; fax: +36 62 433 133.
*E-mail address:* leitgeb@brc.hu (B. Leitgeb).

1093-3263/$ – see front matter © 2009 Elsevier Inc. All rights reserved.
doi:10.1016/j.jmgm.2009.01.005

identify their characteristic structural and conformational features, providing a detailed description of the 3D structure of both conopressins.

## 2. Methods

In order to characterize the conformational spaces and to identify the structural features of Arg-CP-S and Lys-CP-G, simulated annealing calculations were performed with the AMBER 9 software [8] on Fujitsu-Siemens RX220 servers. In the case of SA simulations, the AMBER 99SB force field [9] and the Generalized Born implicit solvent model [10–12] were used, nevertheless, no cut-off was applied for the non-bonding interactions.

After an initial energy-minimization, the following SA procedure was used to explore the conformational spaces of conopressins. The starting geometrically optimized structures were heated up to 1000 K for 1000 fs, then equilibrated at this temperature during 4000 fs, afterwards they were cooled down from 1000 K to 50 K for 10,000 fs. In the course of cooling stage, a multistep (near-exponential) protocol was applied, which was composed of the following three consecutive linear phases: (i) from 1000 K to 500 K through 1000 fs; (ii) from 500 K to 200 K for 2000 fs; (iii) from 200 K to 50 K through 7000 fs. The above-mentioned SA cycle – involving heating, equilibration and cooling stages – was carried out 1000 times for each peptide, thus 1000 conformers were obtained for the conopressins, and all of them were subjected to a final energy-minimization. During this optimization procedure, the steepest descent method was used for the first 100 steps, which was followed by the conjugated gradient algorithm. For the latter, the maximum number of iterations was set to 10,000 and the gradient convergence criterion was set to 0.005 kcal $mol^{-1}$ $A^{-1}$.

Since both conopressins possess a Pro amino acid in position 7, thus it can be considered that these peptides exist as an equilibrium mixture of *cis* and *trans* isomers regarding the $Cys^6$-$Pro^7$ peptide bond. Although, any data about the ratio of the two isomers of Arg-CP-S and Lys-CP-G could not be found in the literature, this *cis–trans* isomerization should be taken into account for the above-mentioned peptide bond, similarly to the case of other peptides containing Xaa-Pro peptide bond [13]. It should be noted that for the γ-CP-vil and L7P-CP-T, the NMR studies indicated the presence of both isomers in solution, namely, the *trans* isomer was observed as major, while the *cis* isomer as minor conformation [6,7]. Accordingly, the *cis* and *trans* isomers of Arg-CP-S and Lys-CP-G were modeled, respectively, applying the appropriate torsional restraints for the $Cys^6$-$Pro^7$ peptide bond (*i.e. cis* isomer: $\omega = 0^\circ$, *trans* isomer: $\omega = 180^\circ$). All other peptide bonds were restrained in *trans* conformation during the SA simulations.

## 3. Results and discussion

### 3.1. Φ–Ψ and $\chi_1$ conformational spaces

To describe the Φ–Ψ conformational spaces in detail and to characterize the distribution of conformers obtained from the SA calculations, Ramachandran (R) and pseudo-Ramachandran (PR) plots, as well as three-dimensional Ramachandran (3DR) and pseudo-Ramachandran (3DPR) plots [14] were constructed. In the case of R and 3DR plots, the $\Phi_i$ and $\Psi_i$ torsion angles of *i*th amino acid were used, while for the PR and 3DPR plots, the $\Phi_i$ torsion angle of *i*th residue and the $\Psi_{i-1}$ torsion angle of $i-1$th residue were applied, in order to produce the Ramachandran plots. To construct the 3DR and 3DPR plots, the ranges of $\Phi_i$ and $\Psi_i/\Psi_{i-1}$ torsion angles (*i.e.* from $-180^\circ$ to $180^\circ$) were divided up into $10^\circ$ intervals, resulting in $36 \times 36$ regions on the $\Phi_i - \Psi_i/\Psi_{i-1}$ conformational spaces. Then, the number of conformers was calculated for all above-mentioned conformational regions, which was represented on the *z*-axis perpendicular to the *x–y* plane, where the *x* and *y* axes relate to the $\Phi_i$ and $\Psi_i/\Psi_{i-1}$ torsion angles, respectively. Applying these 3DR and 3DPR plots, conformational similarity indices ($CS_{XX'}$) [15,16] were calculated, in order to compare the conformational distributions to each other. As four peptides (*i.e. cis* and *trans* isomers of Arg-CP-S and Lys-CP-G) were investigated, thus the $CS_{XX'}$ indices could be represented in $4 \times 4$ lower triangular matrices.

Based on the R and 3DR plots, as well as on the $CS_{XX'}$ indices, the conformational distributions were found to be very similar for the $Ile^3$, $Arg^4$, $Asn^5$ and $Gly^9$ amino acids, respectively, taking into consideration the *cis* and *trans* isomers of both conopressins. In the case of $Ile^2$/$Phe^2$ residues, the above-mentioned plots and indices revealed slightly different distributions of the conformers of Arg-CP-S and Lys-CP-G, which were probably due to the various amino acids located in position 2. However, the R and 3DR plots, as well as the $CS_{XX'}$ indices pointed out the differences observed between the conformational distributions of the *cis* and *trans* isomers of conopressins in the case of $Cys^6$, $Pro^7$ and $Arg^8$/$Lys^8$ residues, severally. Fig. 1 shows the 3DR plots of $Cys^6$, $Pro^7$ and $Arg^8$ amino acids for both *cis* and *trans* isomers of Arg-CP-S, while the $CS_{XX'}$ indices calculated for the residues located in positions 6, 7 and 8 are represented in Fig. 2. The lower triangular matrix of $Cys^6$ amino acid revealed that the $CS_{XX'}$ index was 0.96 for the *trans–trans* and *cis–cis* isomer pairs, whereas the $CS_{XX'}$ indices varied between 0.85 and 0.88 in the case of four pairs including both *cis* and *trans* isomers. In the matrix calculated for the $Pro^7$ residue, the *trans–trans* and *cis–cis* pairs were characterized by the $CS_{XX'}$ indices of 0.97 and 0.98, respectively, while the $CS_{XX'}$ indices existed in the range of 0.63–0.71 for the *cis–trans* and *trans–cis* isomer pairs. The $4 \times 4$ matrix of $Arg^8$/$Lys^8$ amino acids showed the $CS_{XX'}$ indices of 0.9 and 0.91 in the case of *trans–trans* and *cis–cis* pairs, severally, whereas the $CS_{XX'}$ indices varied between 0.79 and 0.84 for the four pairs covering both *cis* and *trans* isomers. The above-mentioned results pointed out a larger difference between the conformational distributions of the *cis* and *trans* isomers of conopressins for the $Pro^7$ residue, compared to the differences observed in the case of $Cys^6$ and $Arg^8$/$Lys^8$ amino acids.

The PR and 3DPR plots, as well as the $CS_{XX'}$ indices indicated that significant differences in the conformational distributions could not be observed in the case of $Cys^1$-$Ile^2$/$Phe^2$, $Ile^3$-$Arg^4$, $Arg^4$-$Asn^5$ and $Arg^8$/$Lys^8$-$Gly^9$ neighbouring residues, severally, considering both *cis* and *trans* isomers of conopressins. These pseudo plots and $CS_{XX'}$ indices showed minor differences in the distributions of the conformers of Arg-CP-S and Lys-CP-G for the $Ile^2$/$Phe^2$-$Ile^3$ adjacent amino acids. This could be explained by the presence of different amino acids in position 2 of the peptides. On the basis of the PR and 3DPR plots, as well as of the $CS_{XX'}$ indices, remarkable differences were detected, concerning the conformational distributions of the *cis* and *trans* isomers of conopressins, for the $Asn^5$-$Cys^6$, $Cys^6$-$Pro^7$ and $Pro^7$-$Arg^8$/$Lys^8$ neighbouring residues, respectively. Fig. 3 represents the 3DPR plots of above-mentioned adjacent amino acids for the *cis* and *trans* isomers of Arg-CP-S, whereas the $CS_{XX'}$ indices with regard to these residue pairs are showed in Fig. 4. In the matrix constructed for the $Asn^5$-$Cys^6$ amino acids, the *trans–trans* and *cis–cis* pairs were characterized by the $CS_{XX'}$ index of 0.88, while for the four pairs covering both *cis* and *trans* isomers, the $CS_{XX'}$ indices were found to be varied between 0.77 and 0.8. The $4 \times 4$ matrix of $Cys^6$-$Pro^7$ residues indicated the $CS_{XX'}$ index of 0.99 in the case of *trans–trans* and *cis–cis* pairs, whereas the $CS_{XX'}$ indices existed in the range of 0.71–0.75 for the *cis–trans* and *trans–cis* isomer pairs. The lower triangular matrix of $Pro^7$-$Arg^8$/$Lys^8$ amino acids showed that the $CS_{XX'}$ index was 0.94 for the *trans–trans* and *cis–cis* isomer pairs, while the $CS_{XX'}$ indices varied between 0.65 and 0.74 in the case of four pairs including

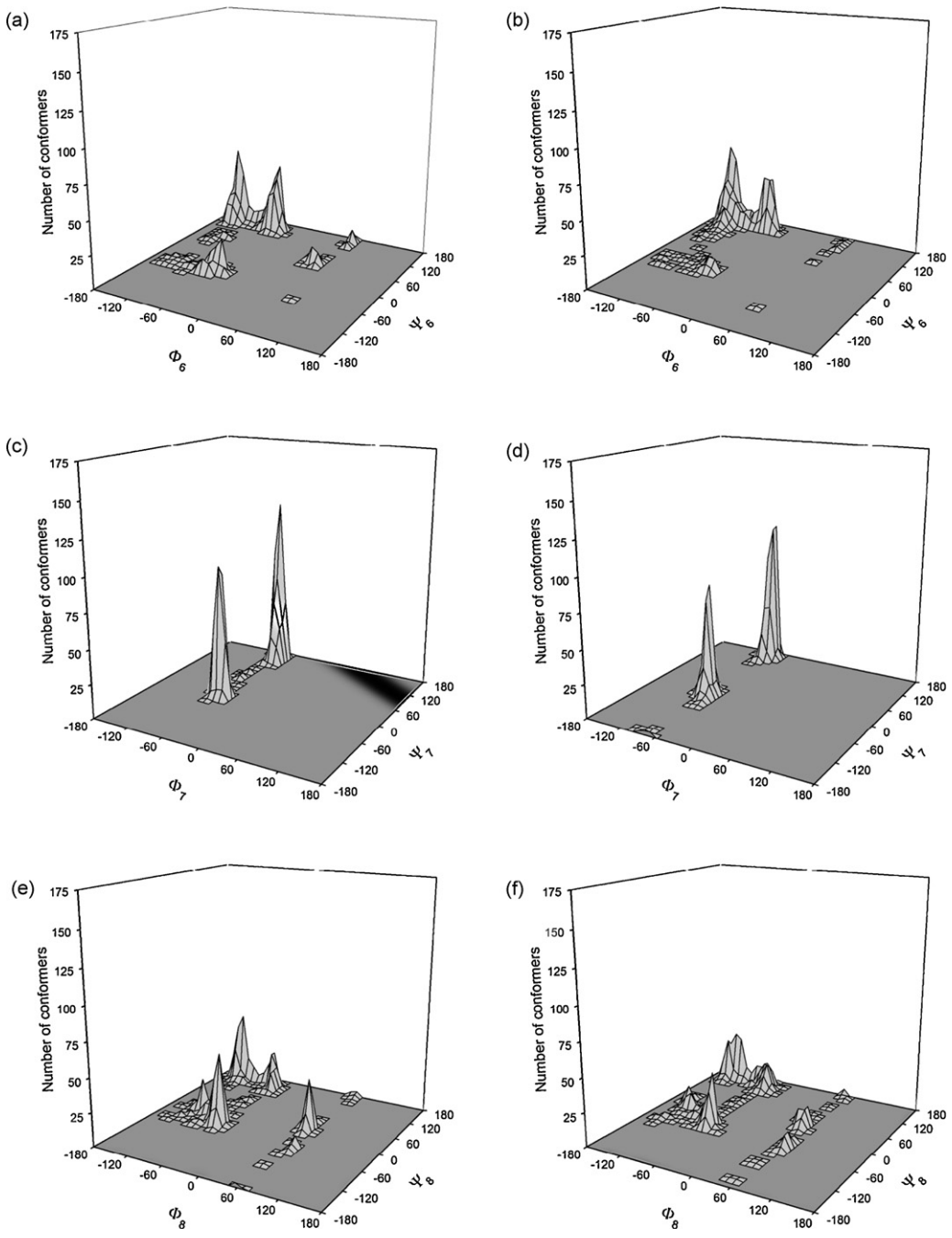


**Fig. 1.** 3DR plots constructed for the Cys[6], Pro[7] and Arg[8] amino acids of the *cis* and *trans* isomers of Arg-CP-S: for the Cys[6] residue of (a) *trans* and (b) *cis* isomers; for the Pro[7] residue of (c) *trans* and (d) *cis* isomers; for the Arg[8] residue of (e) *trans* and (f) *cis* isomers.

both *cis* and *trans* isomers. These results revealed that larger differences could be observed between the conformational distributions of the *cis* and *trans* isomers of conopressins for the Cys[6]-Pro[7] and Pro[7]-Arg[8]/Lys[8] neighbouring residues as compared to those of the Asn[5]-Cys[6] adjacent amino acids.

To characterize the $\chi_1$ conformational spaces, the proportions of $g(+)$, $g(-)$ and *trans* rotamer states were determined, as well as the preferred rotamers were identified for the side-chain of amino acids. Table 1 shows the ratios of three rotamer states for the Cys[1], Ile[2]/Phe[2], Ile[3], Arg[4], Asn[5], Cys[6] and Arg[8]/Lys[8] amino acids of both *cis* and *trans* isomers of conopressins. In the case of the side-chain of Phe[2], Arg[4] and Arg[8]/Lys[8] residues, mainly the $g(-)$ and *trans* rotamers were preferred, while for the side-chain of Ile[2] and Ile[3] amino acids, mostly the $g(+)$ and *trans* rotamers were favored. The side-chain of Asn[5] residues showed a preference for the *trans* rotamer over the two other rotamer states. Although, the side-chain of Cys[1] and Cys[6] amino acids participated in the formation of disulphide bridge, the ratios of rotamers were also determined for these residues, and the results revealed larger proportions of the $g(-)$ and *trans* rotamer states as compared to that of the $g(+)$ rotamer state. Taking into account the *cis* and *trans* isomers of conopressins, significant differences could not be observed with regard to the ratios of three rotamer states for the side-chain of corresponding residues.

### 3.2. Secondary structural elements

For the conformers of both *cis* and *trans* isomers of conopressins, the occurrence of various secondary structural elements was investigated, including different types of β- and γ-turns. The

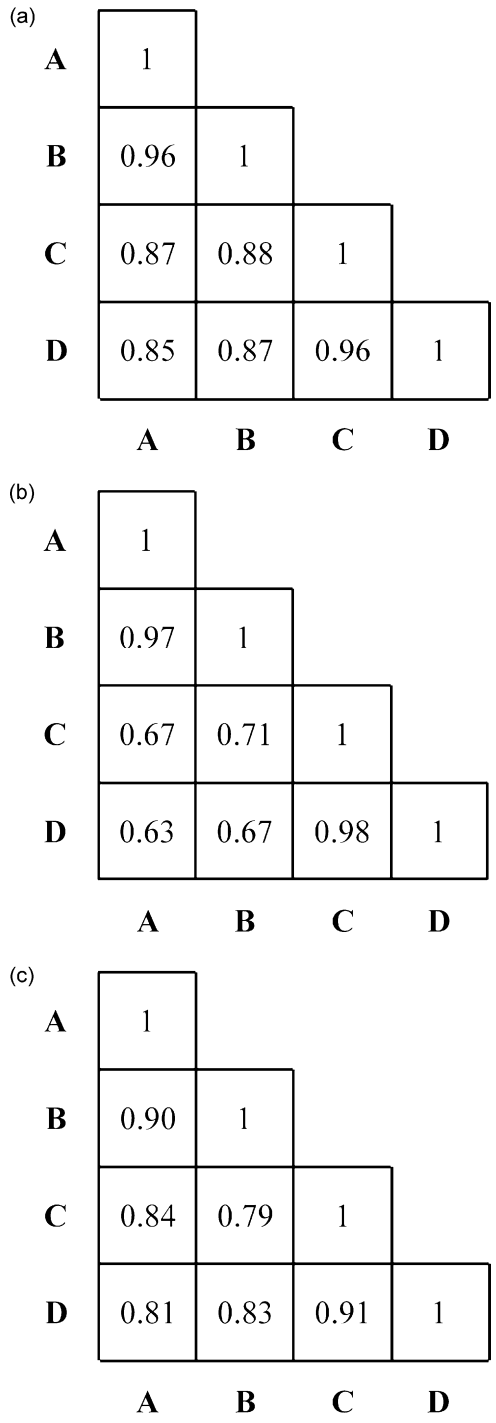


**Fig. 2.** $CS_{XX'}$ indices calculated for the (a) Cys$^6$, (b) Pro$^7$ and (c) Arg$^8$/Lys$^8$ amino acids of conopressins. In the 4 × 4 lower triangular matrices, (A) relates to the *trans*-Arg-CP-S, (B) to the *trans*-Lys-CP-G, (C) to the *cis*-Arg-CP-S and (D) to the *cis*-Lys-CP-G.

β-turn structures were identified according to the characteristic ranges of $\Phi$ and $\Psi$ torsion angles with regard to the $i+1$th and $i+2$th residues of a certain tetrapeptide unit [17–19], which are given in Table 2. To determine the γ- and inverse γ-turns, the following ranges of torsion angles were applied for the $i+1$th residue of a tripeptide segment: (i) for the γ-turn: $\Phi = 70–95^\circ$ and $\Psi = -75$ to $-45^\circ$; (ii) for the inverse γ-turn: $\Phi = -95$ to $-70^\circ$ and $\Psi = 45–75^\circ$ [20–22].

The populations of the different types of β-turns observed in certain tetrapeptide units for the *cis* and *trans* isomers of Arg-CP-S and Lys-CP-G are displayed in Table 3. In the case of both *cis* and *trans* isomers of conopressins, type I and III β-turns were found in the Ile$^2$/Phe$^2$-Ile$^3$-Arg$^4$-Asn$^5$ and Ile$^3$-Arg$^4$-Asn$^5$-Cys$^6$ tetrapeptide units. Additionally, for the *trans* isomer of Arg-CP-S and Lys-CP-G, type I and III β-turns were also detected in the Asn$^5$-Cys$^6$-Pro$^7$-Arg$^8$/Lys$^8$ and Cys$^6$-Pro$^7$-Arg$^8$/Lys$^8$-Gly$^9$ tetrapeptide segments. Although, these β-turns could be observed in the two units mentioned above for the *cis* isomers of conopressins, their populations were smaller compared to those identified for the *trans* isomers. Based on the data presented in Table 3, it could be concluded that in the majority of tetrapeptide segments, the type I β-turns appeared with larger frequency than the type III β-turns, and on the other hand, the populations of both β-turn structures were found to be smaller for the Asn$^5$-Cys$^6$-Pro$^7$-Arg$^8$/Lys$^8$ units in comparison with the populations observed for other three tetrapeptide segments. Nevertheless, in the case of the *trans* isomers of conopressins, a relatively lower amount of type II β-turns (*i.e.* 5.3% for *trans*-Arg-CP-S and 6.1% for *trans*-Lys-CP-G) were detected in the Cys$^6$-Pro$^7$-Arg$^8$/Lys$^8$-Gly$^9$ tetrapeptide units. However, these turn structures were completely absent in the case of the *cis* isomers of conopressins. Beside the afore-mentioned types of β-turns, in the conformers of the *cis* isomer of Arg-CP-S and Lys-CP-G, numerous type VI β-turns (including types VIa1, VIa2 and VIb) were identified in the Asn$^5$-Cys$^6$-Pro$^7$-Arg$^8$/Lys$^8$ tetrapeptide segments (see Table 3). These results are in agreement with the previous observations that the type VI β-turns can generally be observed in tetrapeptide segments of peptides, which contain a Pro amino acid in position $i+2$th, as well as possess a *cis* peptide bond between $i+1$th and $i+2$th residues [18,19]. Among the type VI β-turns, type VIb turn structure was found to be appeared with the largest frequency, in comparison with the occurring populations of type VIa1 and VIa2 β-turns. Moreover, as indicated by the data shown in Table 3, more than half of the conformers of the *cis* isomer of Arg-CP-S and Lys-CP-G possessed one of the above-mentioned type VI β-turns. Based on these observations, it can be concluded that type VI β-turns located in the Asn$^5$-Cys$^6$-Pro$^7$-Arg$^8$/Lys$^8$ tetrapeptide units can be considered as characteristic secondary structural element for the *cis* isomer of both conopressins. However, not only β-turn structures were identified for the conopressins, but inverse γ-turns were also found in the Arg$^4$-Asn$^5$-Cys$^6$ tripeptide segments, and their populations were 9.0%, 6.0%, 5.8% and 7.6% for *trans*-Arg-CP-S, *trans*-Lys-CP-G, *cis*-Arg-CP-S and *cis*-Lys-CP-G, respectively.

On the basis of the afore-mentioned results, it can be seen that a variety of turn structures can be observed in certain tri- or tetrapeptide units of the conformers for both conopressins, which are represented in Fig. 5. Several secondary structural elements appeared in the case of both *cis* and *trans* isomers of Arg-CP-S and Lys-CP-G, such as, type I and III β-turns in the Ile$^2$/Phe$^2$-Ile$^3$-Arg$^4$-Asn$^5$ and Ile$^3$-Arg$^4$-Asn$^5$-Cys$^6$ tetrapeptide units, as well as inverse γ-turns in the Arg$^4$-Asn$^5$-Cys$^6$ tripeptide segments. However, other turn structures were identified, which were found to be characteristic only for one of two isomers, *i.e.*, in the case of *trans* isomers: type I and III β-turns in the Asn$^5$-Cys$^6$-Pro$^7$-Arg$^8$/Lys$^8$ and Cys$^6$-Pro$^7$-Arg$^8$/Lys$^8$-Gly$^9$ tetrapeptide units, as well as type II β-turns in the Cys$^6$-Pro$^7$-Arg$^8$/Lys$^8$-Gly$^9$ tetrapeptide segments; and in the case of *cis* isomers: type VIa1, VIa2 and VIb β-turns in the Asn$^5$-Cys$^6$-Pro$^7$-Arg$^8$/Lys$^8$ tetrapeptide units.

### 3.3. Intramolecular H-bonds

For the conformers of the *cis* and *trans* isomers of Arg-CP-S and Lys-CP-G, the presence of intramolecular H-bonds formed between

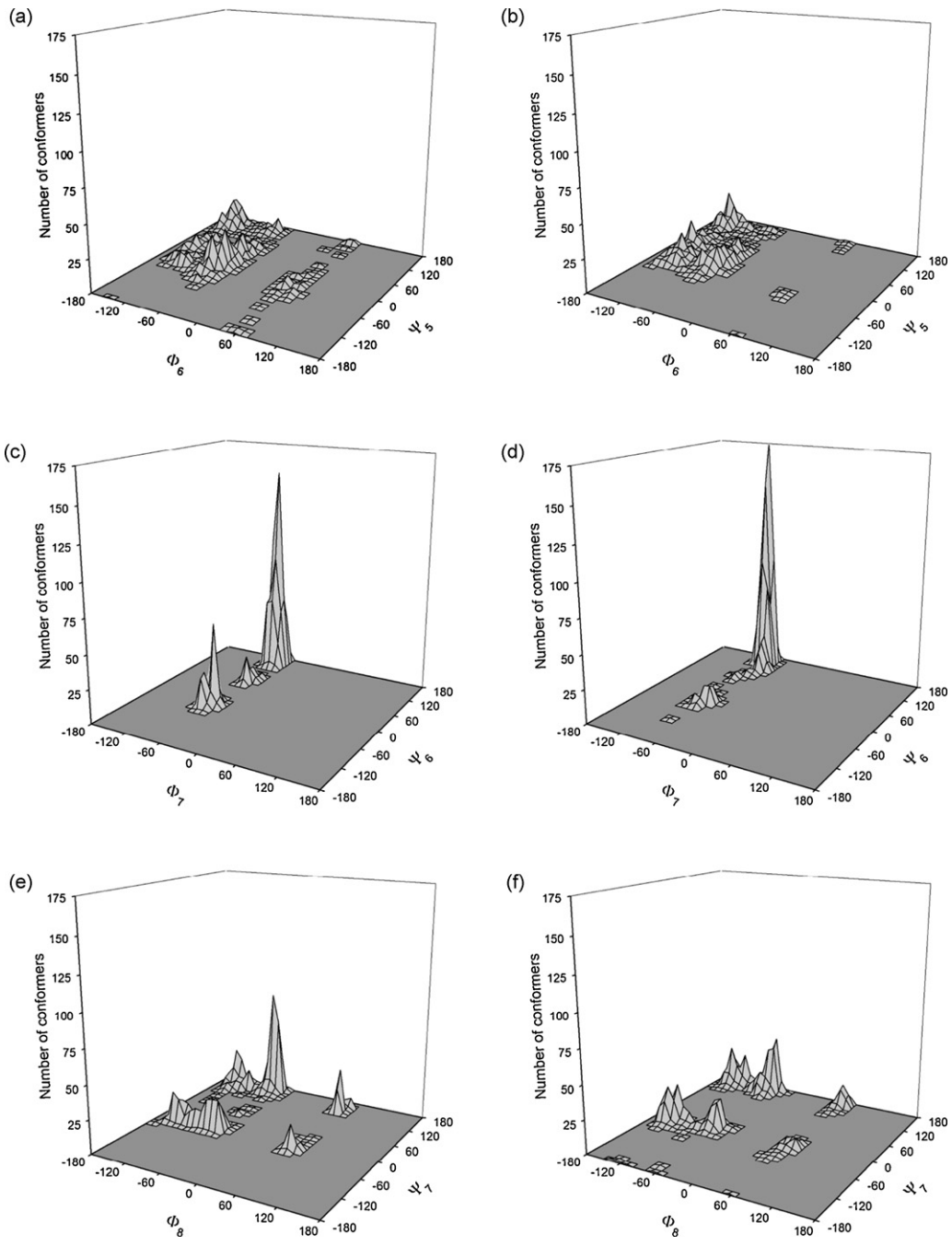


**Fig. 3.** 3DPR plots constructed for the Asn$^5$-Cys$^6$, Cys$^6$-Pro$^7$ and Pro$^7$-Arg$^8$ adjacent amino acids of the *cis* and *trans* isomers of Arg-CP-S: for the Asn$^5$-Cys$^6$ neighbouring residues of (a) *trans* and (b) *cis* isomers; for the Cys$^6$-Pro$^7$ neighbouring residues of (c) *trans* and (d) *cis* isomers; for the Pro$^7$-Arg$^8$ neighbouring residues of (e) *trans* and (f) *cis* isomers.

the backbone NH donor and CO acceptor groups was examined. An intramolecular H-bond was assumed to exist if the $N\cdots O$ distance between the N and O atoms of NH and CO groups was within 3.5 Å, and if the $N–H\cdots O$ angle subtended at the H atom by the bond to the C atom and the line joining the H and O atoms was larger than 120°. Table 4 shows the populations of various intramolecular H-bonds in the case of the *cis* and *trans* isomers of Arg-CP-S and Lys-CP-G.

The majority of turn structures mentioned previously were found to be stabilized by characteristic intramolecular H-bonds. However, several β- and γ-turns were also detected that satisfied the typical $\Phi$ and $\Psi$ torsion angle criteria, but lacked the stabilizing H-bonds, especially for the *cis* isomers of conopressins. The H-bonds between the Ile$^2$/Phe$^2$ and Asn$^5$ amino acids, as well as between the Ile$^3$ and Cys$^6$ residues were observed for both *cis* and *trans* isomers of Arg-CP-S and Lys-CP-G (see Table 4), and these 2 ← 5 and 3 ← 6 H-bonds contributed to the stability of the structure of type I and III β-turns appeared in the Ile$^2$/Phe$^2$-Ile$^3$-Arg$^4$-Asn$^5$ and Ile$^3$-Arg$^4$-Asn$^5$-Cys$^6$ tetrapeptide segments, respectively. In the case of the *trans* isomers of conopressins, the 5 ← 8 and 6 ← 9 H-bonds formed between the Asn$^5$ and Arg$^8$/Lys$^8$ amino acids, as well as between the Cys$^6$ and Gly$^9$ residues were identified (see Table 4), which played a role in the structural stabilization of type I and III β-turns located in

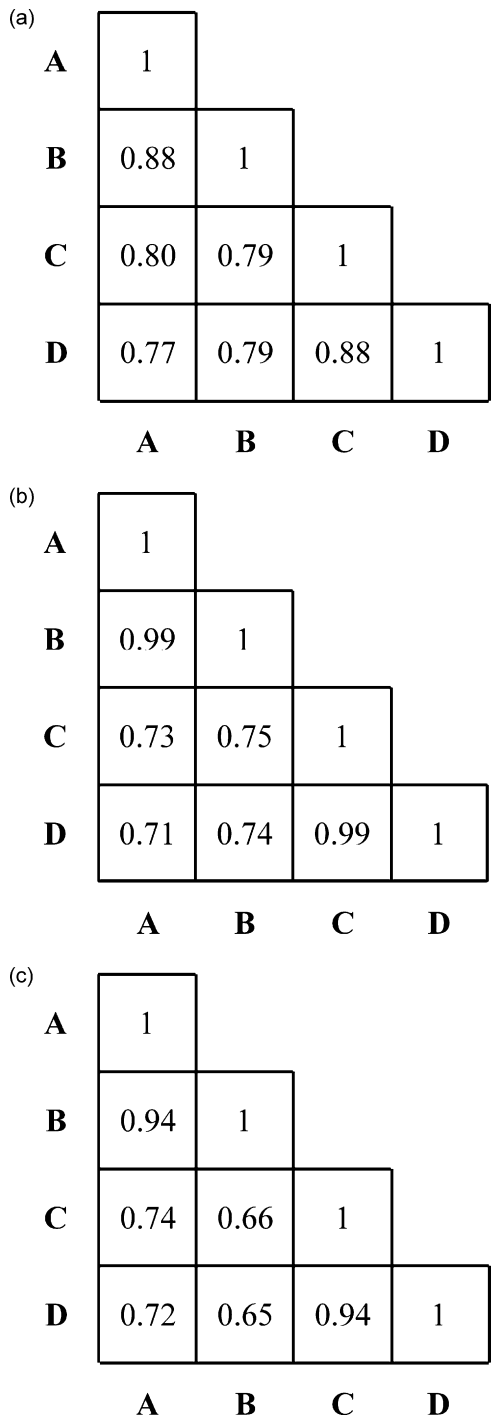


**Fig. 4.** $CS_{XX'}$ indices calculated for the (a) Asn$^5$-Cys$^6$, (b) Cys$^6$-Pro$^7$ and (c) Pro$^7$-Arg$^8$/Lys$^8$ residue pairs of conopressins. In the 4 × 4 lower triangular matrices, (A) relates to the *trans*-Arg-CP-S, (B) to the *trans*-Lys-CP-G, (C) to the *cis*-Arg-CP-S and (D) to the *cis*-Lys-CP-G.

the Asn$^5$-Cys$^6$-Pro$^7$-Arg$^8$/Lys$^8$ and Cys$^6$-Pro$^7$-Arg$^8$/Lys$^8$-Gly$^9$ tetrapeptide units, severally. Furthermore, the 6 ← 9 H-bonds are also important in the stabilization of the structure of type II β-turns observed in the conformers of *trans* isomers. In the case of the *cis* isomers of conopressins, the 5 ← 8 H-bonds appeared with a lower frequency and the 6 ← 9 H-bonds were completely absent (see Table 4), according to the lower amount of type I and III β-turns identified in the above-mentioned two tetrapeptide segments. As described earlier, inverse γ-turn structures were

**Table 1**
Populations (in %) of the $g(+)$, $g(-)$ and *trans* rotamer states for the Cys$^1$, Ile$^2$/Phe$^2$, Ile$^3$, Arg$^4$, Asn$^5$, Cys$^6$ and Arg$^8$/Lys$^8$ amino acids of the *cis* and *trans* isomers of conopressins.

| | *trans*-Arg-CP-S | | | | | | |
|---|---|---|---|---|---|---|---|
| | Cys$^1$-$\chi_1$ | Ile$^2$-$\chi_1$ | Ile$^3$-$\chi_1$ | Arg$^4$-$\chi_1$ | Asn$^5$-$\chi_1$ | Cys$^6$-$\chi_1$ | Arg$^8$-$\chi_1$ |
| $g(+)$ | 23.7 | 45.5 | 41.4 | 17.8 | 15.7 | 22.0 | 21.7 |
| $g(-)$ | 41.4 | 23.0 | 19.7 | 46.1 | 18.6 | 45.0 | 45.2 |
| *trans* | 34.9 | 31.5 | 38.9 | 36.1 | 65.7 | 33.0 | 33.1 |
| | *trans*-Lys-CP-G | | | | | | |
| | Cys$^1$-$\chi_1$ | Phe$^2$-$\chi_1$ | Ile$^3$-$\chi_1$ | Arg$^4$-$\chi_1$ | Asn$^5$-$\chi_1$ | Cys$^6$-$\chi_1$ | Lys$^8$-$\chi_1$ |
| $g(+)$ | 24.5 | 19.3 | 43.4 | 21.1 | 20.9 | 22.8 | 22.1 |
| $g(-)$ | 40.3 | 45.2 | 22.9 | 44.8 | 20.4 | 42.5 | 42.8 |
| *trans* | 35.2 | 35.5 | 33.7 | 34.1 | 58.7 | 34.7 | 35.1 |
| | *cis*-Arg-CP-S | | | | | | |
| | Cys$^1$-$\chi_1$ | Ile$^2$-$\chi_1$ | Ile$^3$-$\chi_1$ | Arg$^4$-$\chi_1$ | Asn$^5$-$\chi_1$ | Cys$^6$-$\chi_1$ | Arg$^8$-$\chi_1$ |
| $g(+)$ | 24.0 | 43.1 | 42.2 | 20.5 | 18.8 | 25.9 | 24.6 |
| $g(-)$ | 38.8 | 19.3 | 21.6 | 46.6 | 22.0 | 38.2 | 36.8 |
| *trans* | 37.2 | 37.6 | 36.2 | 32.9 | 59.2 | 35.9 | 38.6 |
| | *cis*-Lys-CP-G | | | | | | |
| | Cys$^1$-$\chi_1$ | Phe$^2$-$\chi_1$ | Ile$^3$-$\chi_1$ | Arg$^4$-$\chi_1$ | Asn$^5$-$\chi_1$ | Cys$^6$-$\chi_1$ | Lys$^8$-$\chi_1$ |
| $g(+)$ | 24.8 | 16.6 | 45.4 | 18.9 | 19.1 | 29.3 | 23.5 |
| $g(-)$ | 36.8 | 44.0 | 25.0 | 45.6 | 22.9 | 36.4 | 39.8 |
| *trans* | 38.4 | 39.4 | 29.6 | 35.5 | 58.0 | 34.3 | 36.7 |

**Table 2**
Characteristic ranges of the $\Phi$ and $\Psi$ torsion angles regarding the $i+1$th and $i+2$th residues of the different types of β-turns.

| β-turns | $\Phi_{i+1}$ | $\Psi_{i+1}$ | $\Phi_{i+2}$ | $\Psi_{i+2}$ |
|---|---|---|---|---|
| type I β-turn | −60 ± 30° | −30 ± 30° | −90 ± 30° | 0 ± 30° |
| type II β-turn | −60 ± 30° | 120 ± 30° | 80 ± 30° | 0 ± 30° |
| type III β-turn | −60 ± 30° | −30 ± 30° | −60 ± 30° | −30 ± 30° |
| type V β-turn | −80 ± 30° | 80 ± 30° | 80 ± 30° | −80 ± 30° |
| type VIa1 β-turn | −60 ± 30° | 120 ± 30° | −90 ± 30° | 0 ± 30° |
| type VIa2 β-turn | −120 ± 30° | 120 ± 30° | −60 ± 30° | 0 ± 30° |
| type VIb β-turn | −135 ± 30° | 135 ± 30° | −75 ± 30° | 160 ± 30° |

also detected in the Arg$^4$-Asn$^5$-Cys$^6$ tripeptide units for both *cis* and *trans* isomers of Arg-CP-S and Lys-CP-G, which were found to be stabilized by 4 ← 6 typical H-bonds evolved between the Arg$^4$ and Cys$^6$ amino acids (see Table 4). The results mentioned above pointed out that the occurrence of these intramolecular H-bonds is in good agreement with the presence of various turn structures observed in certain tri- or tetrapeptide segments of the conformers of both conopressins.

Beside the afore-mentioned $i \leftarrow i+2$ and $i \leftarrow i+3$ H-bonds, characteristic to the inverse γ-turns and the different types of β-turns, respectively, further intramolecular H-bonds were detected, as indicated in Table 4. These could also play a role in the stabilization of the various conformational states of conopressins. Among the $i \leftarrow i+4$ H-bonds, in the case of the *cis* and *trans* isomers of Arg-CP-S and Lys-CP-G, the H-bonds evolved between the Ile$^2$/Phe$^2$ and Cys$^6$ amino acids were observed, while the H-bonds formed between the Asn$^5$ and Gly$^9$ residues were found in larger number only for the *cis* isomers of conopressins. The C-terminal $NH_2$ group of Arg-CP-S and Lys-CP-G could also participate as donor group in the formation of intramolecular H-bonds. For both *cis* and *trans* isomers of conopressins, the H-bonds between the Pro$^7$ residue and the C-terminal $NH_2$ group were identified, which could contribute to

**Table 3**
Populations (in %) of the type I, III, VIa1, VIa2 and VIb β-turns observed in certain tetrapeptide units for the *cis* and *trans* isomers of conopressins.

| | *trans*-Arg-CP-S | | | |
|---|---|---|---|---|
| | $Ile^2$-$Ile^3$-$Arg^4$-$Asn^5$ | $Ile^3$-$Arg^4$-$Asn^5$-$Cys^6$ | $Asn^5$-$Cys^6$-$Pro^7$-$Arg^8$ | $Cys^6$-$Pro^7$-$Arg^8$-$Gly^9$ |
| type I β-turn | 12.2 | 17.9 | 6.7 | 15.5 |
| type III β-turn | 12.0 | 11.3 | 6.8 | 11.1 |
| | *trans*-Lys-CP-G | | | |
| | $Phe^2$-$Ile^3$-$Arg^4$-$Asn^5$ | $Ile^3$-$Arg^4$-$Asn^5$-$Cys^6$ | $Asn^5$-$Cys^6$-$Pro^7$-$Lys^8$ | $Cys^6$-$Pro^7$-$Lys^8$-$Gly^9$ |
| type I β-turn | 10.8 | 14.8 | 6.0 | 12.5 |
| type III β-turn | 8.9 | 10.1 | 5.7 | 8.8 |
| | *cis*-Arg-CP-S | | | |
| | $Ile^2$-$Ile^3$-$Arg^4$-$Asn^5$ | $Ile^3$-$Arg^4$-$Asn^5$-$Cys^6$ | $Asn^5$-$Cys^6$-$Pro^7$-$Arg^8$ | $Cys^6$-$Pro^7$-$Arg^8$-$Gly^9$ |
| type I β-turn | 10.7 | 15.7 | 1.8 | 2.3 |
| type III β-turn | 9.7 | 9.3 | 2.9 | 5.9 |
| type VIa1 β-turn | – | – | 9.4 | – |
| type VIa2 β-turn | – | – | 9.9 | – |
| type VIb β-turn | – | – | 38.0 | – |
| | *cis*-Lys-CP-G | | | |
| | $Phe^2$-$Ile^3$-$Arg^4$-$Asn^5$ | $Ile^3$-$Arg^4$-$Asn^5$-$Cys^6$ | $Asn^5$-$Cys^6$-$Pro^7$-$Lys^8$ | $Cys^6$-$Pro^7$-$Lys^8$-$Gly^9$ |
| type I β-turn | 10.4 | 15.0 | 1.5 | 3.6 |
| type III β-turn | 7.9 | 7.5 | 1.5 | 6.8 |
| type VIa1 β-turn | – | – | 11.7 | – |
| type VIa2 β-turn | – | – | 9.8 | – |
| type VIb β-turn | – | – | 37.6 | – |

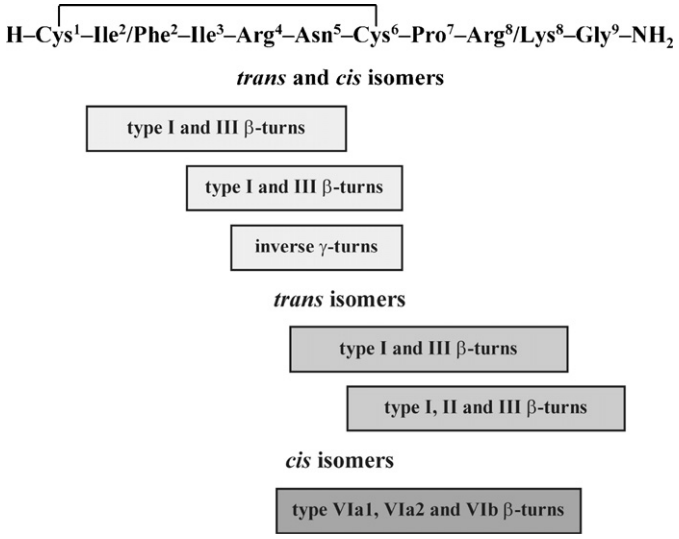


**Fig. 5.** Various turn structures observed in certain tri- or tetrapeptide units for both *cis* and *trans* isomers of Arg-CP-S and Lys-CP-G, as well as for only the *trans* or *cis* isomers of conopressins.

the structural stabilization of the C-terminal tripeptide tail of these conopeptides.

Similarly to the case of turn structures, several intramolecular H-bonds were observed for both *cis* and *trans* isomers of Arg-CP-S and Lys-CP-G, *i.e.*, the $2 \leftarrow 5$ ($Ile^2/Phe^2 \leftarrow Asn^5$), $3 \leftarrow 6$ ($Ile^3 \leftarrow Cys^6$), $4 \leftarrow 6$ ($Arg^4 \leftarrow Cys^6$), $2 \leftarrow 6$ ($Ile^2/Phe^2 \leftarrow Cys^6$) and $7 \leftarrow NH_2$ ($Pro^7 \leftarrow$ C-terminal $NH_2$ group) H-bonds. Nevertheless, another intramolecular H-bonds appeared as characteristic interactions for only the *trans* or *cis* isomers of conopressins, such as, the $5 \leftarrow 8$ ($Asn^5 \leftarrow Arg^8/Lys^8$) and $6 \leftarrow 9$ ($Cys^6 \leftarrow Gly^9$) H-bonds in the case of *trans* isomers, as well as the $5 \leftarrow 9$ ($Asn^5 \leftarrow Gly^9$) H-bonds in the case of *cis* isomers.

**Table 4**
Populations (in %) of the various intramolecular H-bonds for the *cis* and *trans* isomers of conopressins.

| | *trans*-Arg-CP-S | *trans*-Lys-CP-G | *cis*-Arg-CP-S | *cis*-Lys-CP-G |
|---|---|---|---|---|
| $i \leftarrow i+3$ H-bonds | | | | |
| $Ile^2/Phe^2 \leftarrow Asn^5$ | 21.0 | 19.5 | 22.7 | 18.3 |
| $Ile^3 \leftarrow Cys^6$ | 18.9 | 18.2 | 16.9 | 17.6 |
| $Asn^5 \leftarrow Arg^8/Lys^8$ | 5.8 | 5.0 | 1.9 | 2.3 |
| $Cys^6 \leftarrow Gly^9$ | 23.1 | 21.0 | – | – |
| $i \leftarrow i+2$ H-bonds | | | | |
| $Arg^4 \leftarrow Cys^6$ | 13.4 | 11.2 | 10.3 | 13.9 |
| $i \leftarrow i+4$ H-bonds | | | | |
| $Ile^2/Phe^2 \leftarrow Cys^6$ | 11.9 | 9.6 | 14.3 | 11.2 |
| $Asn^5 \leftarrow Gly^9$ | 1.8 | 2.2 | 9.6 | 10.3 |
| H-bonds of the C-terminal $NH_2$ group | | | | |
| $Pro^7 \leftarrow NH_2$ | 14.2 | 14.7 | 12.1 | 12.2 |

## 4. Conclusions

We performed a comprehensive conformational analysis for the Arg-CP-S and Lys-CP-G, focusing on their various structural and conformational features, and our theoretical investigation provided a detailed description of the 3D structure of both conopressins.

In the course of our study, the $\Phi$–$\Psi$ conformational spaces were explored in detail by constructing different types of Ramachandran plots and by calculating $CS_{XX'}$ indices. Additionally, the $\chi_1$ conformational spaces were also characterized via determination of the preferred rotamer states of the side-chain of amino acids. For the Arg-CP-S and Lys-CP-G, the characteristic secondary structural elements were identified, and our results indicated that a variety of turn structures could be observed in certain tri- or tetrapeptide segments of conopressins. Furthermore, typical intramolecular H-bonds were determined, which played an important role in the structural stabilization of the different types of turns. The

occurrence of these H-bonds was in agreement with the presence of turn structures. However, additional intramolecular H-bonds were also detected, which could contribute to the structural stability of the conformational states of Arg-CP-S and Lys-CP-G. The various structural features of the *cis* and *trans* isomers of conopressins were compared to each other, and our results pointed out that several of them appeared for both *cis* and *trans* isomers. Nevertheless, other structural properties were also identified, which were found to be characteristic only for one of the above-mentioned two isomers of conopressins.

To the best of our knowledge, our theoretical study is the first structural investigation performed on the Arg-CP-S and Lys-CP-G, which supply a detailed characterization of the structural and conformational features of conopressins. Moreover, the results derived from our comprehensive conformational analysis might lead to the better understanding of the bioactivity of these conopeptides.

## References


[1] L.J. Cruz, V. de Santos, G.C. Zafaralla, C.A. Ramilo, R. Zeikus, W.R. Gray, B.M. Olivera, Invertebrate vasopressin/oxytocin homologs. Characterization of peptides from *Conus geographus* and *Conus striatus* venoms, J. Biol. Chem. 262 (1987) 15821–15824.

[2] D.B. Nielsen, J. Dykert, J.E. Rivier, J.M. McIntosh, Isolation of Lys-conopressin-G from the venom of the worm-hunting snail, *Conus imperialis*, Toxicon 32 (1994) 845–848.

[3] R.E. van Kesteren, A.B. Smit, R.P.J. de Lange, K.S. Kits, F.A. van Golen, R.C. van Der Schors, N.D. de With, J.F. Burke, W.P.M. Geraerts, Structural and functional evolution of the vasopressin/oxytocin superfamily: vasopressin-related conopressin is the only member present in *Lymnaea*, and is involved in the control of sexual behavior, J. Neurosci. 15 (1995) 5889–5998.

[4] R.E. van Kesteren, C.P. Tensen, A.B. Smit, J. van Minnen, P.F. van Soest, K.S. Kits, W. Meyerhof, D. Richter, H. van Heerikhuizen, E. Vreugdenhil, W.P.M. Geraerts, A novel G protein-coupled receptor mediating both vasopressin- and oxytocin-like functions of Lys-conopressin in *Lymnaea stagnalis*, Neuron 15 (1995) 897–908.

[5] R.E. van Kesteren, C.P. Tensen, A.B. Smit, J. van Minnen, L.F. Kolakowski, W. Meyerhof, D. Richter, H. van Heerikhuizen, E. Vreugdenhil, W.P.M. Geraerts, Co-evolution of ligand-receptor pairs in the vasopressin/oxytocin superfamily of bioactive peptides, J. Biol. Chem. 271 (1996) 3619–3626.

[6] C. Möller, F. Marí, A vasopressin/oxytocin-related conopeptide with γ-carboxyglutamate at position 8, Biochem. J. 404 (2007) 413–419.

[7] S. Dutertre, D. Croker, N.L. Daly, A. Andersson, M. Muttenthaler, N.G. Lumsden, D.J. Craik, P.F. Alewood, G. Guillon, R.J. Lewis, Conopressin-T from *Conus tulipa* reveals an antagonist switch in vasopressin-like peptides, J. Biol. Chem. 283 (2008) 7100–7108.

[8] D.A. Case, T.A. Darden, T.E. Cheatham III, C.L. Simmerling, J. Wang, R.E. Duke, R. Luo, K.M. Merz, D.A. Pearlman, M. Crowley, R.C. Walker, W. Zhang, B. Wang, S. Hayik, A. Roitberg, G. Seabra, K.F. Wong, F. Paesani, X. Wu, S. Brozell, V. Tsui, H. Gohlke, L. Yang, C. Tan, J. Mongan, V. Hornak, G. Cui, P. Beroza, D.H. Mathews, C. Schafmeister, W.S. Ross, P.A. Kollman, AMBER 9, University of California, San Francisco, 2006.

[9] V. Hornak, R. Abel, A. Okur, B. Strockbine, A. Roitberg, C. Simmerling, Comparison of multiple Amber force fields and development of improved protein backbone parameters, Proteins 65 (2006) 712–725.

[10] G.D. Hawkins, C.J. Cramer, D.G. Truhlar, Pairwise solute descreening of solute charges from a dielectric medium, Chem. Phys. Lett. 246 (1995) 122–129.

[11] G.D. Hawkins, C.J. Cramer, D.G. Truhlar, Parametrized models of aqueous free energies of solvation based on pairwise descreening of solute atomic charges from a dielectric medium, J. Phys. Chem. 100 (1996) 19824–19839.

[12] V. Tsui, D.A. Case, Theory and applications of the generalized Born solvation model in macromolecular simulations, Biopolymers (Nucl. Acid. Sci.) 56 (2001) 275–291.

[13] U. Reimer, G. Scherer, M. Drewello, S. Kruber, M. Schutkowski, G. Fischer, Side-chain effects on peptidyl-prolyl *cis*/*trans* isomerisation, J. Mol. Biol. 279 (1998) 449–460.

[14] B. Leitgeb, A. Szekeres, Exploring the conformational space of the μ-opioid agonists endomorphin-1 and endomorphin-2, J. Mol. Struct.: Theochem. 666–667 (2003) 337–344.

[15] D. Pal, P. Chakrabarti, Conformational similarity indices between different residues in proteins and α-helix propensities, J. Biomol. Struct. Dyn. 18 (2000) 273–280.

[16] P. Chakrabarti, D. Pal, The interrelationships of side-chain and main-chain conformations in proteins, Prog. Biophys. Mol. Biol. 76 (2001) 1–102.

[17] C.M. Venkatachalam, Stereochemical criteria for polypeptides and proteins. V. Conformation of a system of three linked peptide units, Biopolymers 6 (1968) 1425–1436.

[18] P.N. Lewis, F.A. Momany, H.A. Scheraga, Chain reversals in proteins, Biochim. Biophys. Acta 303 (1973) 211–229.

[19] K.-C. Chou, Prediction of tight turns and their types in proteins, Anal. Biochem. 286 (2000) 1–16.

[20] B. Leitgeb, G. Tóth, Aromatic–aromatic and proline–aromatic interactions in endomorphin-1 and endomorphin-2, Eur. J. Med. Chem. 40 (2005) 674–686.

[21] E.J. Milner-White, B.M. Ross, R. Ismail, K. Belhadj-Mostefa, R. Poet, One type of gamma-turn, rather than the other gives rise to chain-reversal in proteins, J. Mol. Biol. 204 (1988) 777–782.

[22] E.J. Milner-White, Situations of gamma-turns in proteins, their relation to alpha-helices, beta-sheets and ligand binding sites, J. Mol. Biol. 216 (1990) 385–397.